GRAVIMETRIC AND ELECTROCHEMICAL STUDIES OF *Balanitea egyptiaca* DEL. ETHANOLIC LEAVES EXTRACT AS CORROSION INHIBITOR FOR DUPLEX STAINLESS STEEL (DSS) IN 1.0M HCl SOLUTION

Supported by tetfund

A. I. Onen[1]*, S. Bulama[2], A. M. Kolo[3], E. E. Ebenso[4] and D. A. Apagu[2]
[1]Department of Chemical Sciences, Federal University Wukari, PMB 1020, Taraba State, Nigeria
[2]Department of Chemistry, University of Maiduguri (UNIMAID), Borno State, Nigeria
[3]Department of Chemistry, Corrosion Protection & Material Science Laboratory,
Abubakar Tafawa Balewa University Bauchi (ATBU), Bauchi State, Nigeria
[4]Material Science Innovation & Modelling (MaSIM) Research Focus Area,
North West University, PMB X2046, Mmabatho 2735, South Africa
*Corresponding author: alfredonen@yahoo.com

Received: October 04, 2019 **Accepted:** December 02, 2019

Abstract: The corrosion inhibition performance of *Balanitea egyptiaca* Del. on Duplex stainless steel (DSS) in 1.0M HCl solution was studied by means of gravimetric measurement and Potentio-dynamic polarization techniques. The inhibition efficiency of the inhibitor increased with increasing concentration. From the gravimetric measurements, the inhibitor shows corrosion inhibition efficiency of 96.1% in 50 mg/L concentration at 333K. Polarization studies showed that corrosion current density decreased in the presence of the inhibitor in comparison to the absence of the inhibitor. It also revealed that, the inhibitor acted as a mixed-type inhibitor with inhibition efficiency of 90.6% in 50 mg/L at 303K. The thermodynamic adsorption and activation parameter were evaluated for corrosion inhibition process. The adsorptions of inhibitor on the steel surface obey Temkin adsorption Isotherm. The surface analysis of uninhibited and inhibited steel sample was performed by scanning electron microscope SEM.

Keywords: Gravimetric, Potentio-dynamic polarization, inhibition efficiency, SEM

Introduction

Corrosion phenomena of materials are very complicated in order that corrosion reactions and/or processes depend largely upon the material/environment systems. The damage of the materials caused by the corrosion phenomena has led to the loss in energy and resources, the instability of human life, the decline in the reliability of the infrastructure, and so on. To overcome them, recent advances in the understanding of corrosion phenomena and the mechanism have been introduced. These have led to the development of a higher corrosion resistance material, a more suitable inhibitor and corrosion prevention method, and to a reasonable judgment of the material selection in a given corrosive environment (Nishimura *et al*., 2012).

The corrosion of stainless steel in acidic solutions is one of fundamental academic and industrial concern that have received considerable amount of attention. Stainless steel passivate naturally to form a highly protective film of chromium oxide and is resistant to corrosion in many aggressive environment; however, acidic/chloride solutions are aggressive to this film layer and result in severe pitting formation. Several mineral acid solution are widely used for various treatments of materials in industry such as pickling, descaling acid cleaning and oil well acidizing, thus the presence of corrosion inhibitors is very important to keep the surface of steel intact and reduce their corrosion rate (Roberge, 2000; Baum, 2002; Sharma, 2011).

The use of the inhibitor is one of the best options of protecting metals against corrosion. Several inhibitors in use are either synthesized from cheap raw material or chosen from compounds having hetro-atoms in their aromatic or long chain carbon system. However most of these inhibitors are toxic to the environment. This has prompted the search for green corrosion inhibitors.

Balanitea egyptiaca Del. also known as "Desert date" in English, in Hausa is called Aduuwaa (Roger, 2007) a member of the family zygophyllaceae is one of the most common but neglected wild plant species of the dry land areas of Africa and south Asia (Hall and Waljer, 1991). This tree is native to much of Africa and part of Middle East. In Africa commonly found in Senegal and Sudan. In Nigeria, it is mostly found in the Northern part of the country. In India it is particularly found in Rajasthan Gujarat Madhya, Pradesh and Deccan (Hall, 1992).

It is traditionally used in treatment of various ailments like jaundice, intestinal worm infection, wounds, malaria, syphilis, epilepsy, dysentery, constipation, diarrhea, hemorrhoid, stomach aches, asthma and fever (Daya and Vaghasiya, 2011). The native of Babur-Bura people from Borno State Nigeria, used the leaves to prepare soup called Kavel.

Experimental

Balanitea egyptiaca Del (BA) Leaves Extract Stock Solution

The plant leaf samples were obtained from Bauchi Metropolis along Awala round-about. The leaves were washed with water and air dried in the laboratory and then puverized with pestle and mortar. 100 g were sock in a solution of ethanol for 48 h. After 48 h the sample were filtered and concentrate it by evaporation of the ethanol. The plant extract was used to prepare different concentrations of (10, 20, 30, 40 and 50 mg/L) of the extract in 250 ml of 1.0M HCl for weight loss measurement (gravimetric analysis) and electrochemical measurement.

Duplex Stainless Steel (DSS) Coupon Specimen Preparation

The material used UNS S31803 Duplex stainless steel (DSS) for this study was obtained from ZHEJIAN JIULI HI-TECH Materials Co. LTC china supply by Daewoo E&C (DN57) from Yenegoa, Bayelsa state Nigeria with composition shows in Table 1 below, and were mechanically pressed cut to form different coupons (strips) each were of dimension of 3 x 1 x 0.1 cm (length x breath x thickness). The coupons were carefully polished with SiC paper with different grades (P320, 400, 600, 800 and 1200). Each of the coupons was degreased by washing with ethanol, dried in acetone and preserved in a dessicator for measurement. All reagents used for this study were Analar grade and double distilled water was used for their preparation.

Table 1: Chemical composition of the duplex stainless steel for this study

%C	%Mn	%Si	%S	%P	%Ni	%Cr	%Mo	%N	Fe
0.022	1.270	0.470	0.001	0.025	4.860	22.320	3.050	0.165	67.817

Gravimetric measurements

The gravimetric method employed was earlier reported by Onen *et al*. (2014) for temperatures of 313, 323 and 333K, respectively. The temperatures for each run of the experiments were kept constant using a thermostatic water bath B-scientific England (model HH-W420). In this procedure the weight of the steel coupons was measured using electronic balance B. Brand scientific and instrument company England (model LA 164). The weighed Steel was completely immersed in 250 mL of the test solution containing 1.0M HCl in 250 mL open beaker and Varied masses of the *Balanitea egyptiaca* Del. Leaves extracts (10, 20, 30, 40, and 50 mg) in open beakers. The beakers were immersed into the water bath at the stated temperatures. After every 24 h, each sample was removed from the test solution, washed in a solution of 20% NaOH containing 100 g zinc dust in one liter of distilled water, raised with ethanol and dried in acetone before re-weighing. The difference in weight for a period of 168 hours (7 days) was taken as total weight loss.

From this data, the inhibition efficiency (%I) and the degree of surface coverage (θ) were calculated using Equations (1) and (2)

$$\%I = \left(1 - \frac{W1}{W2}\right) \times 100 \text{ …… (1).}$$

Where W_1 and W_2 are the weight losses (g) for metal in the presence and absence of inhibitor in the test solutions, respectively

$$\theta = \left(1 - \frac{W1}{W2}\right) \text{……. (2).}$$

The corrosion rate in millimeter per year (mm/yr) has been calculated from Equation (3)

$$Corrosionrate(mpy) = \frac{87.6w}{DAT} \text{……. (3)}$$

Where w = weight loss (mg), D = density of specimen (g/cm^3), A = Area of specimen (square meter), T= period of immersion (hour) and 87.6 is a conversion factor. The density of the steel is 7.805 g/cm^3.

Electrochemical measurements

Steel electrode were cut from the mechanical pressed used in for weight lost measurement of thickness 0.1 cm the electrode were of dimension 1 X 1 cm^2 and were weld from the one side to a copper wire used for electric connection and was mounted in epoxy resin to expose geometrical surface area of 1 cm^2. Prior to these measurements the expose surface was pretreated in the same manner as for weight loss experiments.

Potentiodynamic polarization measurements

Several methods may be used in polarization of specimens for corrosion testing. Potentio-dynamic polarization is a technique where the potential of the electrode is varied at a selected rate by application of a current through the electrolyte. It is probably the most commonly used polarization testing method for measuring corrosion resistance and is used for a wide variety of functions (Ousslin *et al*., 2013).

The electrochemical experiments were carried out in three electrode electrochemical cylindrical pyrex glass cell with the platinum counter electrode and saturated calomel electrode (SCE) as reference at 303K. The working electrode had the form of a square cut the steel (1 cm^2). The exposed area was treated as before. A duration time 30 min was given for the system to attain a steady state and the open circuit potential (OCP) was noted. Both cathodic and anodic polarization curve were recorded potentio-dynamically by changing the electrode potential between -1.5V and +1.5V at the scan rate of 1mV/s. The percentage inhibition efficiency were calculated from the electrochemical measurement by Equation (4)

$$(\eta\%) = \frac{i^o_{corr} - i_{corr}}{i^o_{corr}} \times 100 \text{ … … … (4)}$$

Scanning electron microscope

The scanning electron microscope photographs were recorded at 1000 x magnification at accelerating voltage of 15kV using Phenom Pro X SEM model, Netherlands.

Results and Discussion

Table 2 shows the values of percentage inhibition efficiency, corrosion rate and surface covered of the steel in 1.0M HCl with the different concentrations of the inhibitor. The inhibition efficiency and surface covered increases with the increase in concentrations for either temperatures studied for the experiment but decreases with increase in temperature from 313 to 333 K.

Table 2: Corrosion parameters for DSS corrosion in 1.0M HCl with inhibitor at 313, 323, and 333K

Inhibitor conc.(mg/L)	Percentage inhibition efficiency (%I)			Corrosion rate (mm/yr)			Surface coverage (θ)		
	313K	323K	333K	313K	323K	333K	313K	323K	333K
Blank	-	-	-	22.961	29.491	30.912	-	-	-
Balaniteaegyptiaca									
10	48.40	27.20	14.40	11.848	21.469	26.460	0.484	0.272	0.144
20	61.40	42.40	20.50	8.863	16.987	24.575	0.614	0.424	0.205
30	67.70	56.10	29.90	7.370	12.947	21.669	0.677	0.561	0.299
40	78.60	60.70	37.80	4.914	11.590	19.227	0.786	0.607	0.378
50	96.10	71.80	42.20	0.950	8.316	17.867	0.961	0.718	0.422

This is as a result of the binding effect of the adsorbed inhibitor (desorption taking place) hence inhibition efficiency and surface covered decreases. Increase in corrosion rate is observed as the temperature increased in both the acid solution without and with inhibitor. It may also be observed that an addition of an increased concentration of the inhibitor generally retarded the corrosion rate of the steel in the acid solutions. This is also seen and supported from the decreasing change in mass loss taking place with an increase in inhibitor concentration in Fig. 1.

Effect of inhibitor concentration on inhibition efficiency

Inhibition efficiency were determined using Equation (1) and reported in Table 2. Fig. 2 shows plot of inhibition efficiency versus various concentrations of the inhibitor of **BA** at 313, 323, and 333K. Inhibition efficiency increase with increase concentration but decreases with temperature increases. This shows that the inhibitor function effectively at lower temperature (313K). This trend of inhibition effectiveness is also confirmed from the polarization studies (Table 5). The decreases in inhibition efficiencies with increasing temperature show that the time lag for the process of adsorption of the inhibitor molecules on the DSS surface becomes shorter. This observation is in agreement with report by Onen *et al.* (2011) and Kolo *et al*. (2017).

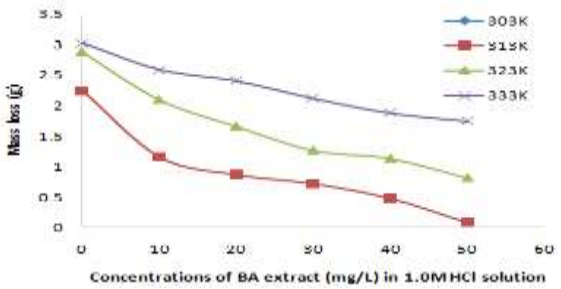

Fig. 1: Plot of mass loss (g) of DSS against 1.0M HCl and various concentration of inhibitor BA at 313, 323 and 333K

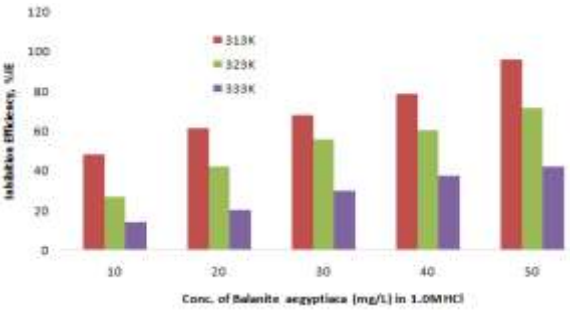

Fig. 2: Plot of percentage inhibition efficiency (%I_E) of DSS against various concentration of inhibitor (BA) at 313, 323 and 333K

Thermodynamic and activation parameters

Values of activation energy for the corrosion reaction of DSS in the presence and absence of different concentration of the BA leaves extract have calculated using the Arrhenius Equation (5);

$$CR = Ae^{\frac{Ea}{RT}} - - - - - - - - (5)$$

Taking the logarithm of both side of equation (5) and (6) is obtained;

$$logCR = logA - \frac{Ea}{2.303RT} - - - - - - - (6)$$

Where CR is the corrosion rate of DSS (equation 3), A is Arrhenius constant, E_a is the activation energy of the reaction, R is the gas constant (8.314 J/mol K) and T is the temperature.

A plot of log CR verses 1000/T (Fig. 4) it will a straight line from the slope the value of E_a was calculated and show in Table 3.

It is evident from Table 3, that the values of the apparent activation energy for the inhibited solutions were higher than that for the uninhibited solutions. The higher values of apparent activation energy (E_a) in the presence of inhibitor as compare to the E_a in the absence of inhibitor in 1.0M HCl solution indicated that the inhibitor induces the energy barrier for the corrosion reaction which leads to the decreasing of rate of corrosion of DSS in the present of inhibitor (Dehri and Ozcan, 2006).

The values of standard enthalpy of activation ΔH^* and standard entropy of activation ΔS^* where calculated using erring equation of transition state as;

$$CR = \frac{RT}{Nh}\exp\left(\frac{\Delta S^*}{R}\right)\exp\left(\frac{-\Delta H^*}{RT}\right) \quad \text{-------} (5)$$

Where h is planck's constant and N is the Avogadro's number, respectively.

A plot of log (CR/T) against 1000/T (Fig. 4) gave straight lines with a slope of $\frac{-\Delta H^*}{2.303R}$ and an intercept of $\left[log\frac{R}{Nh} + \frac{\Delta S^*}{2.303R}\right]$, from which the activation thermodynamics parameters ΔH^* $and \Delta S^*$ were calculated, as listed in Table 3.

Table 3: Activation parameter for DSS in 1.0M HCl solution in the absence and presence of inhibitor obtained from weight loss measurement

Inhibitor	Concentration (mg/L)	Ea ($kJmol^{-1}$)	ΔH^* ($kJmol^{-1}$)	ΔS^* ($kJmol^{-1}$)
Blank	-	12.83	1.34E-02	-63.45
BA	10	34.85	8.43E-02	-63.24
	20	44.39	1.11E-01	-63.15
	30	47.09	1.12E-01	-63.13
	40	59.34	1.16E-01	-57.87
	50	129.78	1.39E-01	-51.11

The negative value of ΔS^* indicates that the formation of the activated complex in the rate determining step represents an association rather than a dissociation step, meaning that a decrease in disorder take place during the causes of the transition from reactant to activated complex (Wang *et al*., 2011).

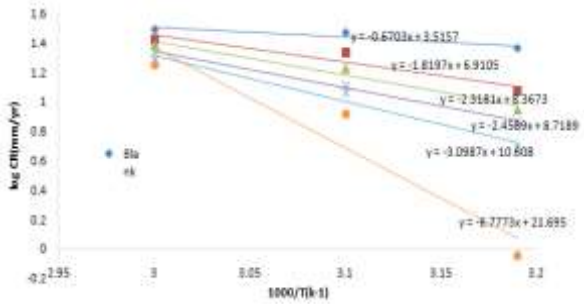

Fig. 3: Arrhenius plot of log CR versus 1000/T for DSS corrosion in 1.0M HCl solution BA extract

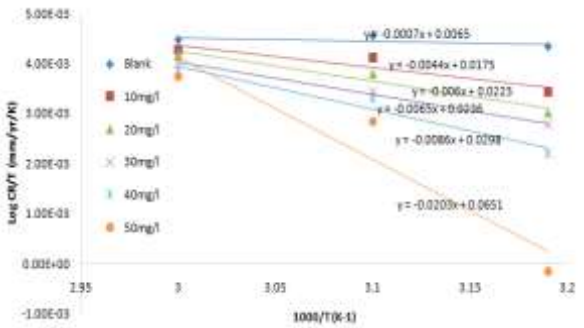

Fig. 4: Transition state plot of log CR/T versus 1000/T for DSS in 1.0M HCl solution at different concentration of BA extract

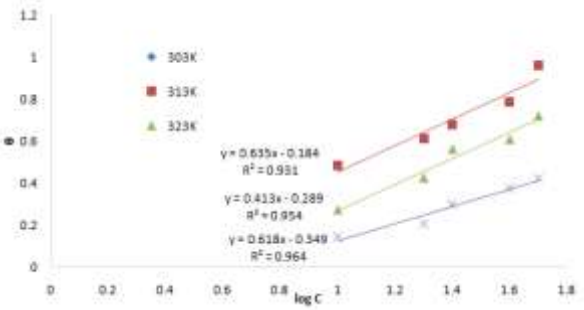

Fig. 5: Plot of Temkin adsorption isotherm for DSS in inhibitor BA at 313, 323 and 333 K

Adsorption isotherm

Adsorption isotherms are important in understanding the mechanism of inhibition of corrosion reactions. Various isotherm models with two or three parameters are available for modeling equilibrium data. Two-parameter isotherms are the most commonly used isotherms because of their simplicity

and possibility of linearization. However transformation of non-linear isotherm models to linear forms usually results in parameter estimation error. Three parameter isotherms have three adjustable parameters and cannot be estimated by linear regression (Sharma *et al*., 2010).

The adjustable parameters of all isotherms analyzed here were calculated using linear regression analysis. In order to describe the goodness-of-fit of the experimental data to the proposed models, the correlation coefficient (R^2) was calculated. The entire adsorption isotherm can be represented as follow:

$$f(\theta, x)\exp(-2a\theta) = kC - - - - - (6)$$

Where $f(\theta, x)$ is the configuration factor which depends upon the physical model and the assumption underlying the derivation of the isotherm.θ Is the degree of surface coverage, C is the inhibitor concentration in the electrolyte, x is the size ratio, a is molecular interaction parameter, and k is the equilibrium constant of the adsorption process. The adsorption behavior of the BA extract as a green corrosion inhibitor has been analyzed for the Frumkin, Temkin and Flory-Huggins adsorption isotherms. It was found that the Temkin adsorption model was the best fit with correlation coefficients above 0.9313 for the temperatures studies. While others correlated at less than 0.73.

The Temkin isotherm is given by equation (7);

$$\theta = -\frac{2.303}{2a}logK_{ads} - \frac{2.303}{2a}logC - - - - (7)$$

The mathematically implication of equation (7) is that a plot of θ versus $logC$ produce a straight line with slop and intercept equal to $-\frac{2.303}{2a}$ and $-\frac{2.303}{2a}logK_{ads}$, respectively.

A plot of θ versus $logC$ (Fig. 3 is obtained for the adsorption of BA extract onto DSS was linear with correlation co-coefficient (R^2), slope and intercept as presented in Table 4. These suggest that the adsorption obey Temkin.

The equilibrium constant of adsorption K_{ads} is related to the standard free energy of adsorption ΔG^o_{ads} with the following equation (8)

$$\Delta G^o_{ads} = -2.303RTlog(55.5K_{ads}) - - - - - (8)$$

Where R is the molar gas constant, T is the absolute temperature and 55.5 is the concentration of water in solution expressed in molar

Table 4: Isotherm parameters for the adsorption of inhibitors on DSS surface at 313, 323, and 333 K in 1.0M HCl

Adsorp. Isotherm	Inhibitor	Temp. (K)	Intercept	Slope	K_{ad}	*A*	−ΔG (kJ/mol)	R^2
Temkin	BA	313	-0.1842	0.6350	0.513	-1.81	8.71	0.9313
		323	-0.2895	0.4137	0.242	-2.45	6.97	0.9544
		333	-0.3497	0.6187	0.272	-1.86	7.36	0.9640

Adsorp. = Adsorption, Temp. = Temperature

The standard free energy of adsorption was calculated using equation 8 and the values obtained were presented in Table 4. It can be seen from the values reported that the standard free energy reflects a spontaneous reaction that has physisorption mechanism at temperatures studied. (Standard free energy negatively less than threshold value of -40 kJ/mol) (Bouklah *et al*., 2013).

The values of the lateral intermolecular parameter (a) were found to be negative values which indicate that a slight decrease in the adsorption energy take place with increase in surface coverage. In addition intermolecular interaction between adsorbed molecules is minimal (El-Awady *et al*., 1992).

Polarization studies

The effect of addition of inhibitor on the anodic and cathodic polarization curve of DSS in 1.0M HCl solution was studied and polarization curves are shown in Fig. 6 at 303K. The values of cathodic (β_c) and anodic (β_a) Tafel slops were calculated from the linear region of the Polarization curves. The corrosion current density (i_{corr}) was determined from the intersection of the linear part of the anodic and cathodic curves with the open circuit corrosion potential (E_{corr}). The corrosion parameters such as corrosion potential (E_{corr}), anodic Tafel slope (β_a), cathodic Tafel slope(β_c), corrosion current density (i_{corr}) and the percentage inhibition efficiency (I%) obtained from the curve are given in Table. 5.

The result reveal that increasing concentration of inhibitor resulted in a decrease in current densities, corrosion rate and increase in inhibition efficiency, suggesting the adsorption of inhibitor molecules at the surface of the DSS form a protective film on DSS surface. This assertion conforms to an earlier report by Yadev *et al*. (2016). The presence of inhibitor cause change in E_{corr} values with respect to theE_{corr} in absence of inhibitor.

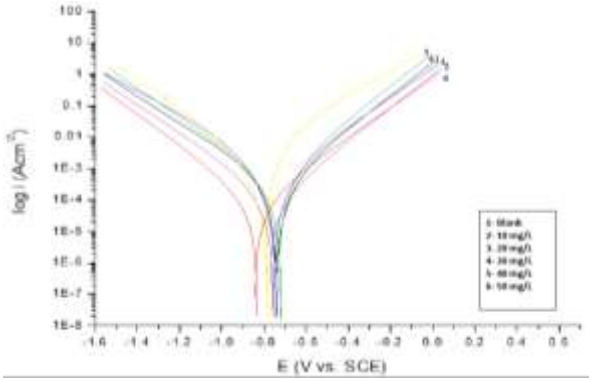

Fig. 6: Potentiodynamic polarization curve for DSS in 1.0M HCl solution in the presence and absence of BA as inhibitor at 303K

Table 5: Electrochemical parameters and percentage inhibition efficiency obtained from polarization studies for DSS in 1.0M HCl solution in the absence and presence of inhibitors at 303K

Inhibitor	Conc (mg/l)	$-E_{corr}$ (mV/SCE)	i_{corr} (μA/cm²)	$-\beta_a$ (mV/dec	$-\beta_c$ (mV/dec⁻¹)	%I	CR (mm/yr)
Blank	-	762	274	417	189	-	3.18
BA	10	756	205	277	334	25.2	1.22
	20	731	172	387	326	37.2	1.11
	30	724	132	243	311	52.0	1.01
	40	793	43.7	425	241	84.1	0.85
	50	833	25.8	716	109	90.6	0.30

If the displacement in E_{corr} in presence of inhibitor is more than $\pm 85mV/SCE$ relating to E_{corr} of the blank, the inhibitor can be considered as a cathodic or anodic type. If the change in E_{corr} is less than $\pm 85mV/SCE$ the corrosion inhibitor may be regarded as a mixed type. This implies that the inhibitor act as mixed type inhibitor affecting both anodic and cathodic reaction. The maximum displacement in our study is 71 mV/SCE which agrees with the findings of Yadev *et al.* (2015).

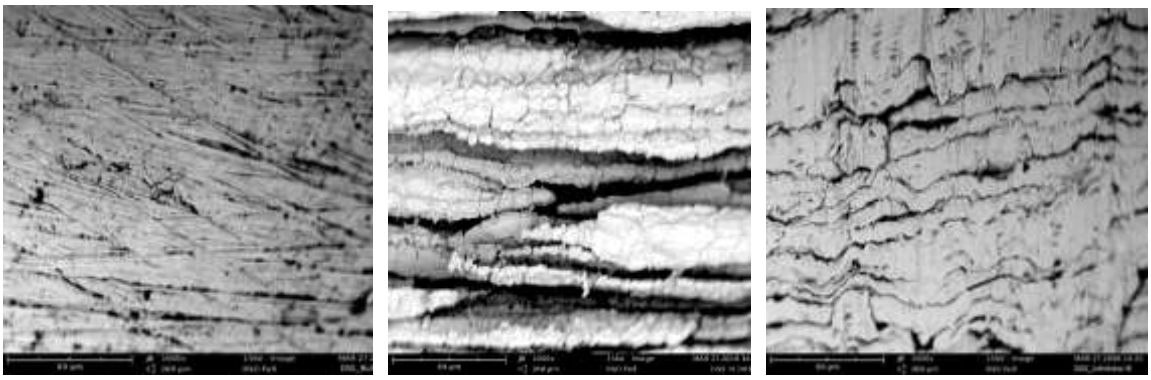

(a) Polished steel **(b) Steel in 1.0M HCl** **(c) Steel in 1.0M HCl with the inhibitor**

Fig. 7: Showing the polished steel, steel in 1.0M HCl and steel in 1.0M HCl in the presence of inhibitor

Scanning Electron Microscope (SEM)

Figure 7(a, b, and c) shows scanning electron micrograph of the polished DSS, DSS in 1.0M HCl, and DSS 1.0M in the presence of BA extracts, respectively. A severe corrosion can be observed in the absence of the inhibitor (b). However in the presence of inhibitor (c), show that the steel surface is partially covered with inhibitor which further proves to some extent that BA act as a good inhibitor at 1.0M HCl acid concentration.

Conclusion

The BA extract investigated in this paper act as good corrosion inhibitor for DSS in 1.0M HCl solutions. The gravimetric and electrochemical measurements confirm the inhibitive nature of the BA extract. Inhibition efficiency increases with increasing the extract concentration and decreases with rise of the temperature. It's exhibited a maximum inhibition efficiency of 96.1% for gravimetric measurement and 90.6% for electrochemical measurement. Potentio-dynamic studies reveal that, the inhibitor act as a mixed type. In addition its inhibition proceeded via the mechanism of a physical absorption and spontaneously in nature (ΔG^{o}_{ads} values were less than the threshold value of -40 kJ/mol) and was best described by Temkin adsorption model. The SEM images of the inhibited strips reveal the likely formation of protective firm.

References

Baum P 2002. Guide lines on metals and alloys used as food contact materials. Council of Europe's 13 – 21.

Bouklah M, Kaddari M, Toubi M, Hammouti B, Radi S & Ebenso EE 2013. Corrosion inhibition of steel in Hydrochlric acid solution by new N N'-Bipyrazole piperazine Derivative. *Int. Jour.electrochem. Sci*., 8: 7437-7454.

Daya LE & Vaghasiya HU 2011. A review on *Balaniteaegyptiaca Del*. (Desert date) Phytochemical constituents, traditional uses and phytochemcial activity. *J. Pharm.*, 5(9): 55-56.

Dehri I & Ozcan M 2006. The effect of temperature on the corrosion of mild steel in acidic media in the presence of some sulphur containing organic compounds. *J. Mater. Chem. Phys*., 98(2-3): 316-323.

El-Awady AA, Ab-el-Nasey BA & Aziz SG 1992. Kinetic-Thermodynamic and Adsorption Isotherms analysis for inhibition of the acid corrosion of steel by cyclic and open-chain Amines. *J. Electrochem. Soc.*, 139(8): 2149-2154.

Hall JB & Waljer DH 1991. *Balaniteaegyptiaca Del*. School of Agricultural and Forest science Banger: University of Wales, pp. 1-12.

Hall JB 1992. Ecology of a key African multipurpose tree species *Balaniteaegyptiaca Del.* The state of knowledge forest ecol. *Manag*., 50: 1-30.

Kolo AM, Kutama IU, Sani UM & Usman U 2017. Electrochemical, SEM and FTIR study of the corrosion inhibition of *Januvia* for Zinc in Hydrochloric acid medium. *J. Appl. Chem. Sci. Int.*, 6(4): 210-216.

Nishimura R, Tsuru T, Ohtsuka T, Hara N, Han E & Alyousif O 2012. Understanding of Corrosion Phenomena Process, Mechanism and Method. *Int. J. Corros.* Article ID 286174. 1-2

Onen AI, Maitera ON, Joseph J & Ebenso EE 2011. Corrosion inhibition potential and adsorption behavior of bromophenol blue and thymol blue dyes on mild steel in acidic medium. *Int. J. Electrochem. Sci*., 6: 2884-2897.

Onen AI 2014. The behavior of *Moraceaefiscusglumosadelile* as a corrosion inhibitor for Zinc in H_2SO_4. *Chem. Sci. Rev. Let.*, 3(115): 49-55.

Ousslin A, Chetauani A, Hammounti B, Bekkouch K, Al-Deyab SS, Aoutiniti A & Elidrisssi A 2013. Thermodynamic quantum and electrochemical studies of corrosion of iron by piperazine compounds in sulphuric acid. *Int. J. Electrochem. Sci*., 8: 5980-6004.

Roberge PR 2000. Handbook of Corrosion Engineering. McGraw-Hill 2-6

Roger B 2007. Hausa names for plant and trees. 2nded Circulation version 2-5.

Sharma SK, Mudhoo A, Jain G & Sharma J 2010. Corrosion inhibition and adsorption properties of *Azadirach taindica* mature leaves extract as green inhibitor for mild steel in HNO_3. *Green Chem. Lett. and Rev.* 3(1): 7-15.

Sharma BK 2011. Industrial Chemistry" 6thed Krishna, pp. 1697-1732.

Wang X, Yang H & Wang F 2011. An investigation of benzimidazole derivatives as corrosion inhibitor for mild steel in different concentration HCl Solution. *J. Corros. Sci.*, 53: 113-121.

Yadev M, Kumar S, Kumari N, Bahadur I & Ebenso EE 2015. Experiment and Theoritical studies on corrosion inhibition effect of synthesized Benzothiazole derivative of Mild steel in 15% HCl solution. *Int. J. Electrochem. Sci.*, 10: 602-624.

Yadev M, Gope L, Kumari N & Yadev P 2016. Corrosion inhibition performance of pyranopyrazole derivative for mild steel in HCl solution: gravimetric, electrochemical and DFT studies. *J. Mol. Liq.*, 216: 78-86.